PERGAMON

International Journal of Heat and Mass Transfer 42 (1999) 4207–4224

International Journal of HEAT and MASS TRANSFER

www.elsevier.com/locate/ijhmt

Three-dimensional pore network simulation of drying in capillary porous media

Y. Le Bray, M. Prat*

Institut de Mécanique des Fluides de Toulouse, UMR CNRS-INP/UPS No. 5502, avenue du Professeur Camille Soula, 31400 Toulouse, France

Received 4 December 1997; received in revised form 3 December 1998

Abstract

Results of a three-dimensional pore network simulation of drying under constant external conditions are reported. It is shown that the pore network drying model capture specific features of drying of capillary porous media such that the phenomenon of dry patches and the occurrence of a constant rate period (CRP). These phenomena are explained as consequences of the fractal invasion percolation patterns that characterize drying when the capillary forces dominate. The evolution of the liquid phase structure within the pore network during drying is studied and the process of fragmentation of the liquid phase into isolated clusters is analysed. The various periods of the drying curve are analysed from the evolution of the liquid phase distribution within the sample.

1. Introduction

Despite the huge amount of literature devoted to drying of capillary porous media, several features of drying are still puzzling. For example, Van Brakel [1], mentions in his review that dry and wet patches can be recognized at the surface of a porous medium during drying. Explanation for the formation of such patches is not given, however. Nothing is presented regarding the size and the evolution of the patches. Also, under constant external conditions, a constant drying rate period (CRP) is generally observed, Van Brakel [1]. Various explanations of the CRP have been given in the past. According to Van Brakel, the most convincing explanation is due to Suzuki and Maeda [2]. These authors have shown that a CRP could occur if the size of wet and dry patches on the surface is small compared to the thickness of the external mass boundary layer. However, in the analysis of Suzuki and Maeda and in the review of Van Brakel, no attempt was made to show that the size of the patches occurring during drying was indeed consistent with this result. In presenting the analysis of Suzuki and Maeda, Van Brakel assumes that the size of the patches is on the order of the pore or grain size. This is in fact in complete disagreement with the experimental results reported in Maneval [3]. Using NMR imaging techniques, Maneval obtained two-dimensional local scale saturation distributions during drying of a pack of glass beads. The size of the surface heterogeneities was clearly much greater than the bead diameter. Therefore, it should be concluded that there is in fact no satisfactory explanation of the CRP. Maneval's results indicate, however, that a better understanding of the liquid phase distribution within the porous medium and at the surface during drying is a necessary first step towards an explanation of the dry and wet

* Corresponding author. Tel.: 0033 561 285877; fax: 0033 561 285878.

E-mail address: prat@imft.fr (M. Prat)

0017-9310/99/$ - see front matter
PII: S0017-9310(99)00006-X

Nomenclature

CRP	constant rate period	h	mass transfer coefficient (kg/m^2/s/Pa)
FRP	falling rate period	L	network size (m)
RCP	receding front period	m	normalized drying rate
BT	breakthrough (first percolation transition)	P_{vi}	vapor partial pressure at the interface (Pa)
MCD	main cluster disconnection (second percolation transition)	$P_{v\infty}$	reference vapor partial pressure (Pa)
c	evaporation flux density (kg/m^2/s)	σ	standard deviation of the vapor partial pressure distribution at the interface

patches phenomenon as well as the CRP. In this article, those questions are investigated through three-dimensional pore network simulations. To the best of our knowledge, this is the first time that three-dimensional pore network simulations of drying are presented. The pore network drying model used for the simulations, Prat [4], has been extensively used for studying drying in two-dimensional systems, Prat [5], Laurindo and Prat [6,7]. Comparisons with experimental results for transparent etched networks, Laurindo and Prat [6,7], have shown that this drying model was a very appropriate tool for studying the phase distribution evolution during drying at the pore network scale. This model is briefly presented in the next section. It is perhaps worth mentioning, however, that there exist essential differences between drying in two-dimensions and drying in three-dimensions that prevent the occurrence of a CRP for two-dimensional systems and therefore impose to study the CRP with three-dimensional porous media. As explained in previous works [5–9], the slow drying process investigated in the present article is essentially an invasion percolation process where secondary invasions occur in the liquid trapped clusters that forms during drying. It is well known [10], that trapping changes the invasion percolation quite drastically in two-dimensions. Trapping is important in two-dimensions but negligible in three-dimensions during the first stages of the invasion. For this reason, a CRP is observed in three-dimensions but not in two-dimensions.

2. Drying model

The objective is to simulate the evaporation of a liquid from an initially saturated capillary porous medium, as sketched in Fig. 1. The simulator is described in detail in previous articles [4–6]. Additional details can also be found in Laurindo [8] and Le Bray [9]. Its main features are the following. The pore space is modelled by a simple cubic lattice of sites and bonds (or throats) of various sizes. The width of each bond is randomly chosen according a uniform distribution law in the range 0.1–0.7 mm. Initially, the network is completely saturated by a single component liquid. The boundaries of the network are formed by six surfaces. Vapor escapes through one of these six surfaces, this is the top surface in Fig. 2. The other surfaces are impervious.

The phenomena taken into account are the capillary effects modelled by means of the invasion percolation rules [10], the phase-change at each elementary liquid–gas interface, and the diffusive transport in the gas phase. The gas phase is a binary mixture made up of the vapor of the liquid and an inert component. Heat transfer is not taken into account. As only capillary porous media are considered, the Kelvin's effect is neglected. As discussed in our previous articles, the capillary effects result in the occurrence of many liquid clusters as in standard invasion percolation. Computing the evaporation at the boundary of each cluster present in the system helps to solve the problem of diffusive transport of the vaporized species through the gas phase at each step of the invasion. As explained by Prat [14], it is also possible to include the

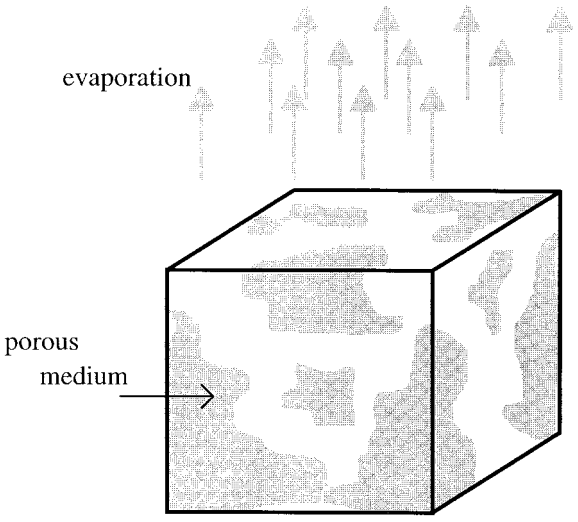

Fig. 1. Configuration studied.

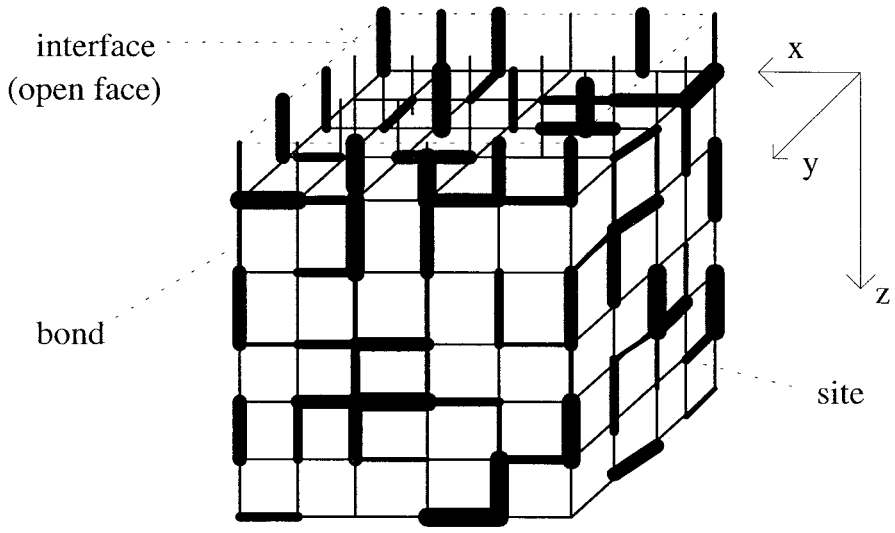

Fig. 2. The model porous medium considered (simple cubic network).

gravity effects by defining an appropriate invasion throat potential depending on the width of the throat, the relative position of the throat in the gravity field, and the Bond number, that is the ratio of the gravity forces to the capillary forces. In the present article, however, gravity effects are not taken into account. As explained by Prat [5], the present model is valid in the limit of very low capillary numbers (quasi-static limit), that is when capillary effects dominate. This is a very reasonable restriction, since drying is a very slow process under usual laboratory conditions.

The mass transfer at the open surface is modelled by means of a local constant mass transfer coefficient, that is the local liquid vapor flux density is expressed as

$$e = h(P_{vi} - P_{v\infty}) \tag{1}$$

in which h and $P_{v\infty}$ are the local mass transfer coefficient and the reference vapor partial pressure in the gas phase surrounding the network respectively and P_{vi} is the liquid vapor partial pressure at the entrance of the considered bond at the open boundary of network. It has been shown elsewhere [11], that drying is in fact a (heat and) mass transfer conjugate problem which needs to solve simultaneously the external transport equations and the equations of the drying model for the porous materials. As a result the interfacial transfer coefficients are generally not constant. Solving the drying problem as a conjugate problem by coupling the pore network model and some external transport model is, however, very CPU time demanding and has not been attempted in the present study. This attractive line of attack, called in the following the conjugate approach, will undoubtedly be used in the future for studying the mass transfer at the interface. As mentioned before, we proceeded simply by assuming a local constant mass transfer coefficient. It should be stressed that such an assumption is conservative with regard to the model of Suzuki and Maeda [2] and the conjugate approach. In the model of Suzitki and Maeda [2], the transport along the surface contributes to make the vapor pressure uniform at a short distance from the interface within the external mass boundary layer. Due to this effect, a partially wet surface may behave as it were completely wet. This effect will be present also in a conjugate approach. When a local constant transfer coefficient is used, this effect is not incorporated. Therefore, if the present model leads to a CRP, we will be able to conclude that a CRP would inevitably be observed in the more realistic conjugate approach. As mentioned before, the present model is valid in the quasi-static limit (very low capillary number). Therefore, throughout this article, drying and drainage will always be considered under the assumption of a very low capillary number.

3. Simulations

The results presented in this article were obtained for a $51\times 51\times 51$ network. Because of the CPU time required for a full simulation of drying (several days on a IBM RS 6000/375 workstation) only one realisation of network was considered.

3.1. Drying periods

Three drying periods are usually distinguished from

the drying curve: the so-called constant drying period (CRP), the falling rate period (FRP) and the receding front period (RFP) [1]. An idea would be to relate those different periods drawn from a typical drying curve to changes in terms of the phase distribution structure within the porous domain. In drainage at low Ca, which can be described by invasion percolation, two particular stages of invasion are usually distinguished: (i) the breakthrough (BT) when the injection fluid reaches the outlet for the first time, and (ii) the terminal point when the displacement stops. Breakthrough represents the percolation threshold of the non-wetting phase, while with trapping, the terminal point represents the percolation threshold of the wetting phase. At the terminal point, the wetting phase is distributed within the system in the form of disconnected clusters. Thus, in drainage, the wetting fluid, which initially forms a single cluster occupying the whole pore space, gets progressively broken up into clusters of various sizes until the terminal point is reached. It has been shown elsewhere [5,6] that drying and drainage at low Ca lead to the same invasion sequence of the main (infinite) cluster, that is, the wetting fluid cluster which is connected to the outlet in drainage, and is connected to the impervious surface corresponding to the drainage outlet in drying (this is the bottom surface in Fig.1). Therefore, what is known about drainage, in terms of the phase distribution evolution, represents a first approximation of the phase distribution evolution in drying. As shown by Prat [5] and Laurindo and Prat [6], this is, however, only a first approximation, because in drying, the disconnected liquid clusters that form during the process are invaded owing to evaporation at the boundary of these clusters (due to the liquid incompressibility, those clusters cannot be invaded in drainage). Furthermore, it is clear that the breakthrough and the terminal point, which are important moments of drainage, are not necessarily associated with some particular stage of drying. Therefore, it is necessary to explore specifically the evolution of the phase distribution in drying.

3.2. Global behavior

First insights can be gained from numerical visualizations of the liquid–gas interface within the network during drying as shown in Fig. 3. Three main stages can be distinguished. In the first stage the gas preferentially invades the region of the open face. Irregular fractal patterns typical of invasion percolation are obtained as shown in Fig. 3a and 3b. The second stage is characterized by an invasion of the sample which seems statistically homogeneous and isotropic (this is clearly evidenced in the numerical animation from which Fig. 3a–h were selected). A typical visualization for this stage is shown in Fig. 3c. As can be seen from Fig. 3d–h, the third stage is characterized by the full drying of the sample through an evaporation process sweeping the network from the open (top) face to the bottom face. Disconnected clusters are clearly visible in Fig. 3e–h. This suggests that the liquid phase is in fact distributed in the form of disconnected clusters when the third stage starts. Hence, in terms of phase distribution evolution, drying can be defined as a progressive fragmentation and erosion process of the liquid phase. Initially, the liquid phase forms a single cluster spanning the network. When the third phase starts, there is no network spanning liquid cluster anymore but a large number of isolated liquid clusters of various sizes. This suggests to define as a 'critical' step of drying, the main cluster disconnection (MCD), which is the moment where for the first time there is no liquid cluster completely spanning the network, that is, connecting the open and the 'outlet' face. In other terms, at MCD, the largest liquid cluster (termed hereafter the main cluster) is no longer connected to the open face. This step corresponds to a percolation transition [12].

3.3. Saturation profiles

Fig. 4 shows the evolution of the saturation profiles along the z axis. The saturations depicted in Fig. 4 are the average saturation over x–y slices. The three main stages described above can be clearly seen in Fig. 4, that is, the initial stage that ends a little after 'breakthrough', the second stage marked by an isotropic and homogeneous invasion, and the third stage which resembles a receding front period. Note, however, end-effects during the second stage in the open and bottom face regions. It is interesting to observe that the saturation in the first slice (saturation at the interface) varies much more during the first and third stages than during the second stage where it stabilizes in the range 0.3–0.35. In others terms, Fig. 4 indicates that the relative change in the overall saturation is much greater than the relative change in the saturation at the interface during a significant part of the second stage.

Fig. 5 shows the evolution of the slice average saturations as a function of the overall saturation. End effects can be seen in Fig. 5. Before MCD, the saturation gradient along z is much greater for the first three and last three slices than in the remaining part of network. Three phases can be distinguished in Fig. 5. The first phase up to BT is characterized by the spreading of the slice average saturation along z. Between BT and MCD, the slice average saturations become more and more uniform in the bulk of the network. During the third phase after MCD two regions are present in the system: a dry region, and an unsaturated region in which the saturation is uniform with a sharp transition between the two regions. The dry

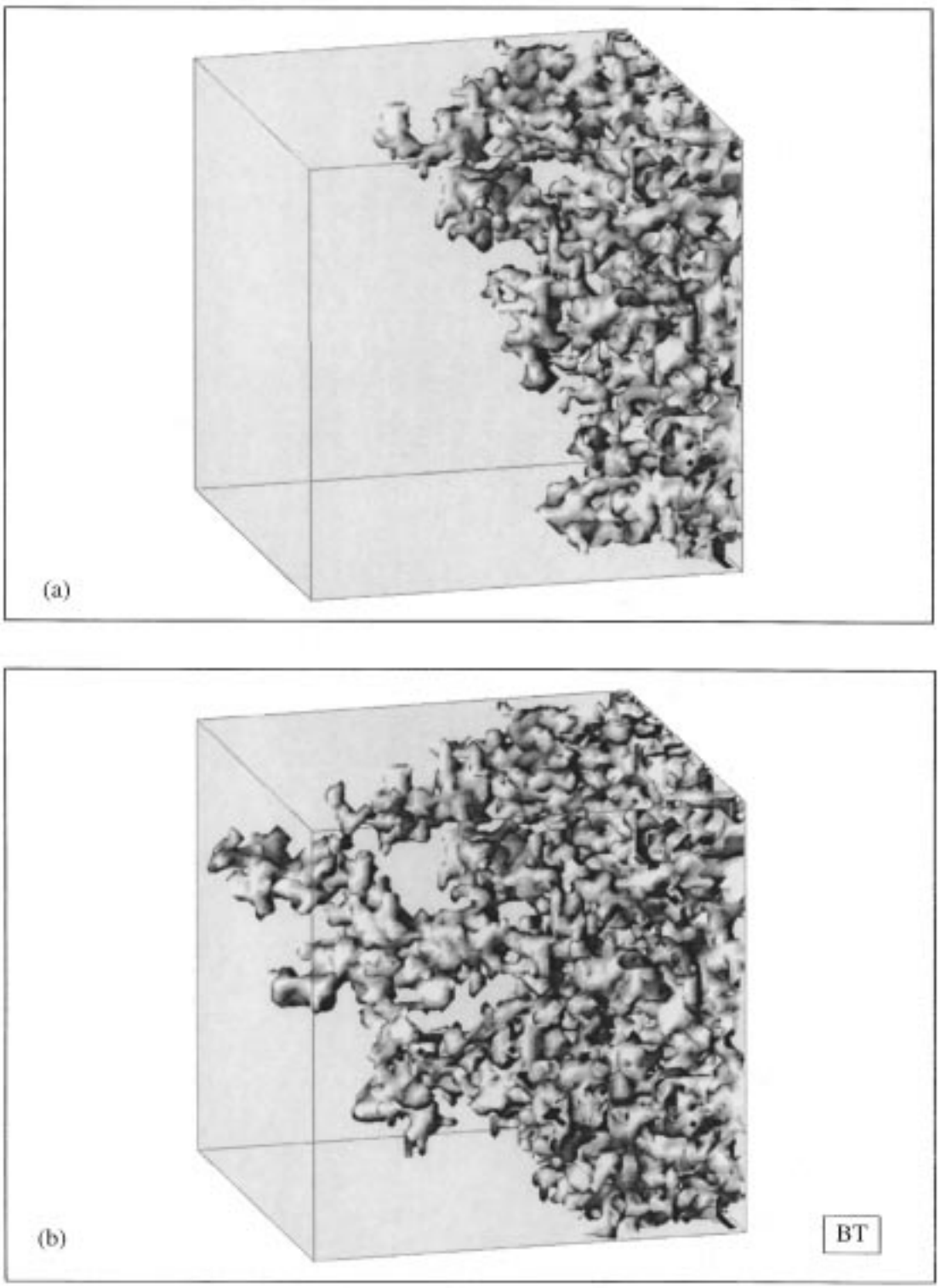

Fig. 3. Evolution of the liquid–gas interface within the network during drying. The top (open) face of Fig. 1 corresponds to the (hidden) right-hand face in the figure. The bottom face in Fig. 1 corresponds to the left-hand face in the figure.

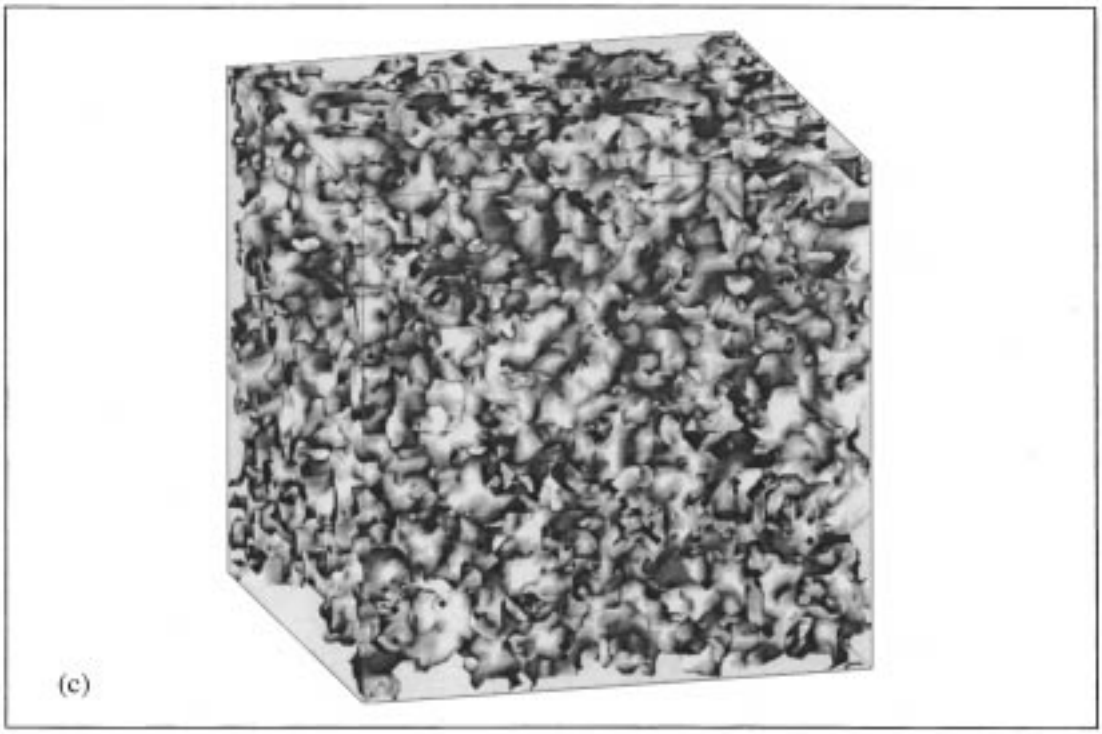

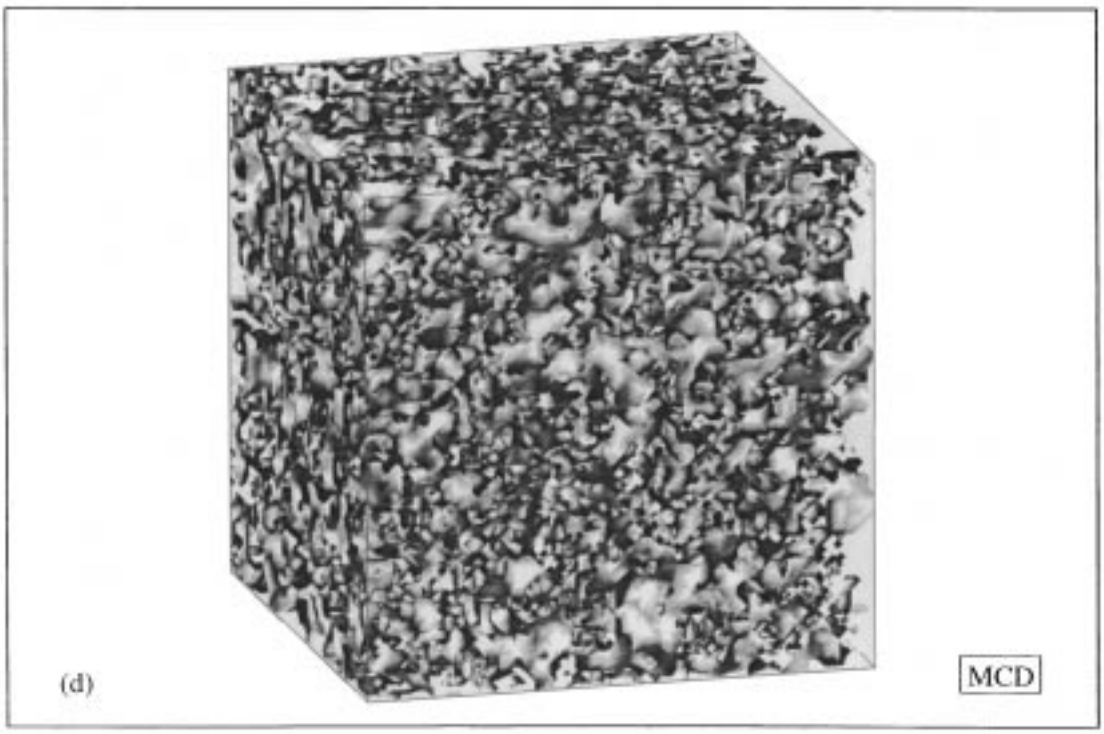

Fig. 3 (*continued*)

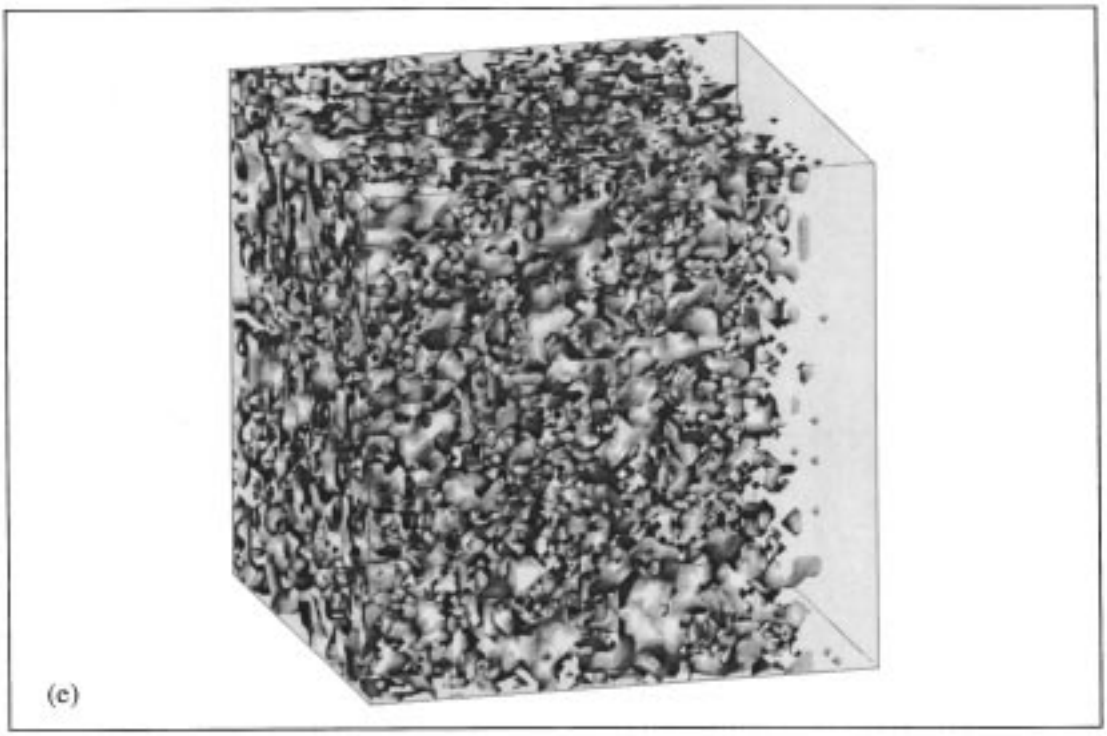

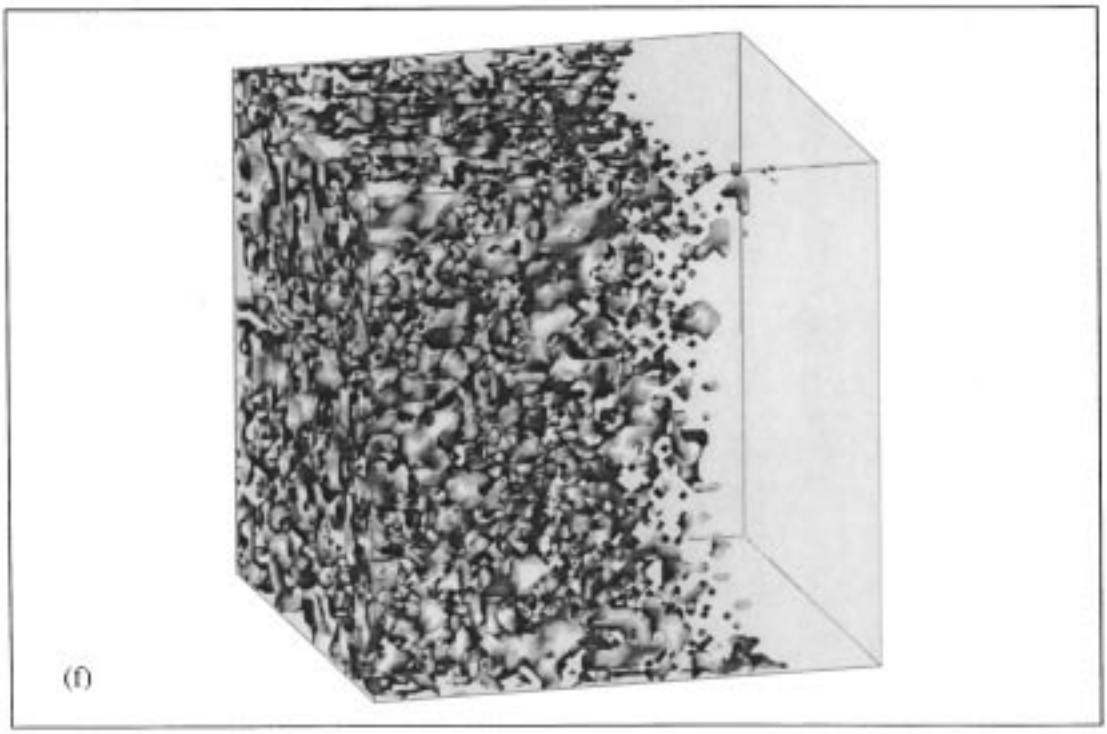

Fig. 3 (*continued*)

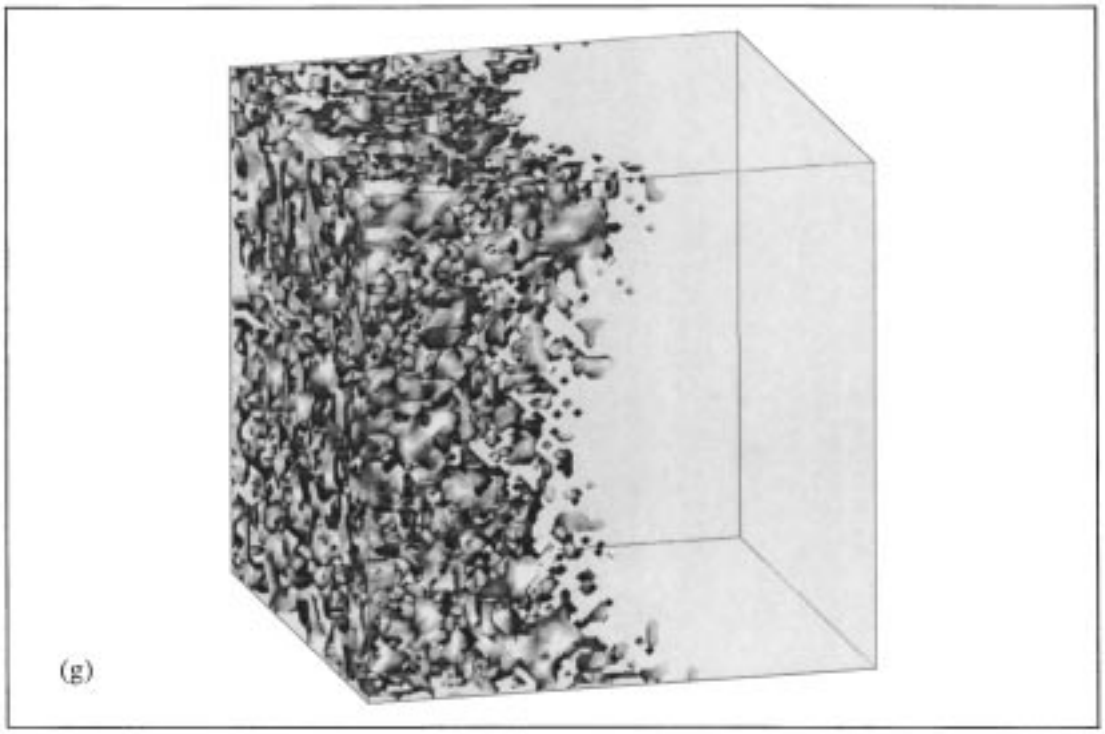

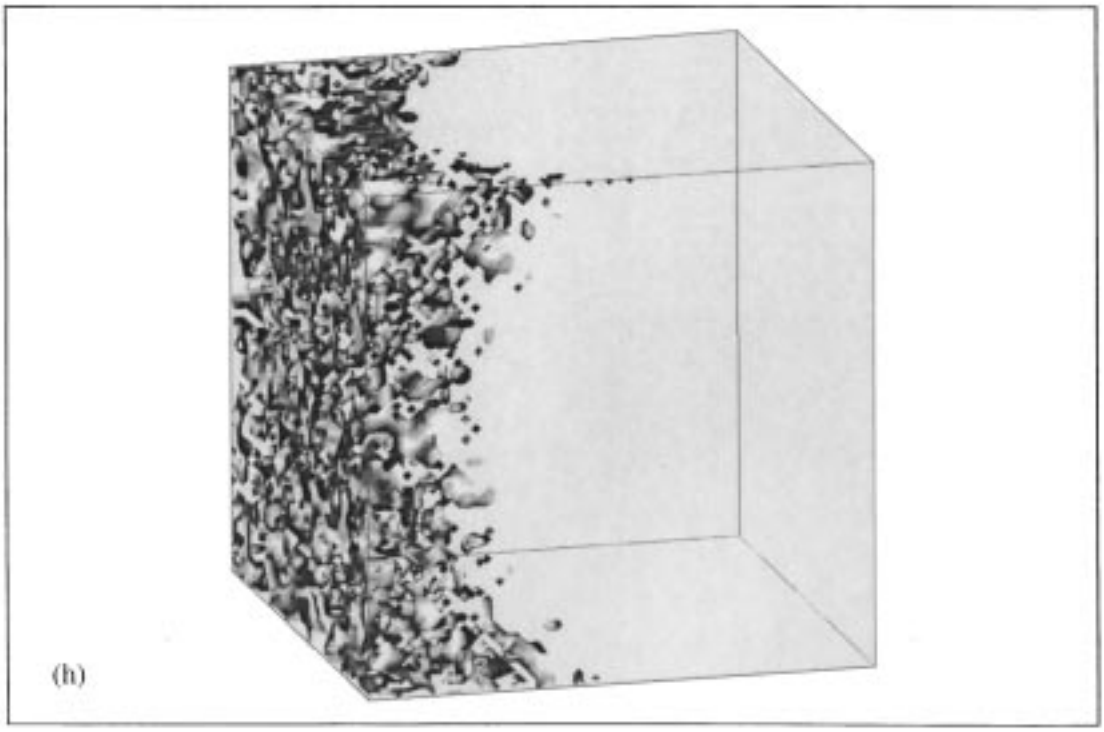

Fig. 3 (*continued*)

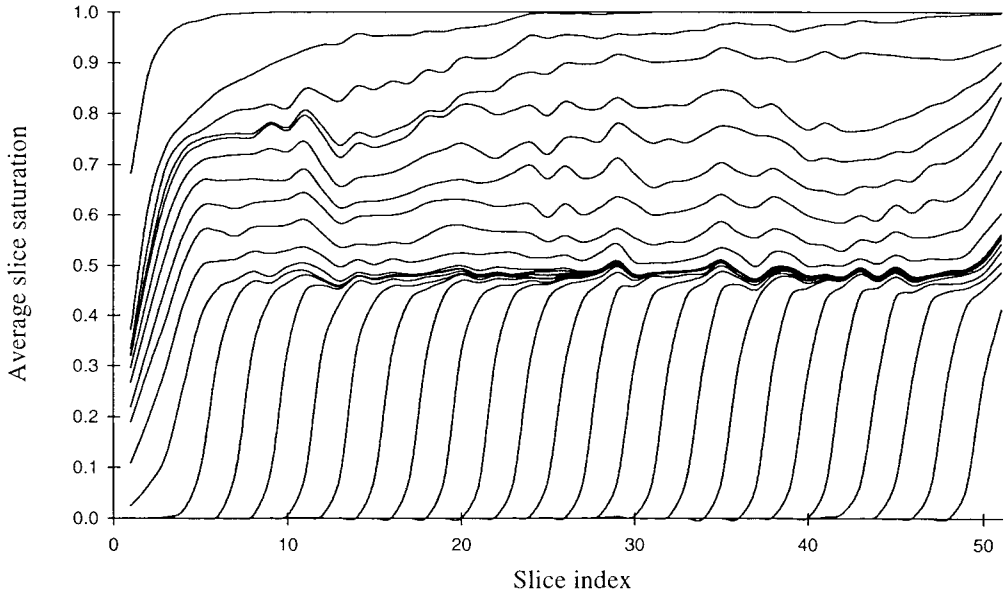

Fig. 4. Slice averaged saturation profiles at various times along z. Slice no. 1 corresponds to the open face of network, slice no. 51 to the bottom face of network.

region extension grows during this last phase. Fig. 5 also shows that there is no direct relation between the surface saturation and the overall saturation. Therefore, this questions the relevance of approach in which the mass transfer coefficient is considered as function of the overall saturation, see for example Kaviany and Mittal [13] among others.

3.4. Liquid cluster evolution

The question considered in this section is how the liquid phase progressively becomes broken into disconnected clusters. As can be seen from Fig. 6 the number of cluster first increases and reaches a maximum shortly after MCD. Fig. 7 compares the clusters distri-

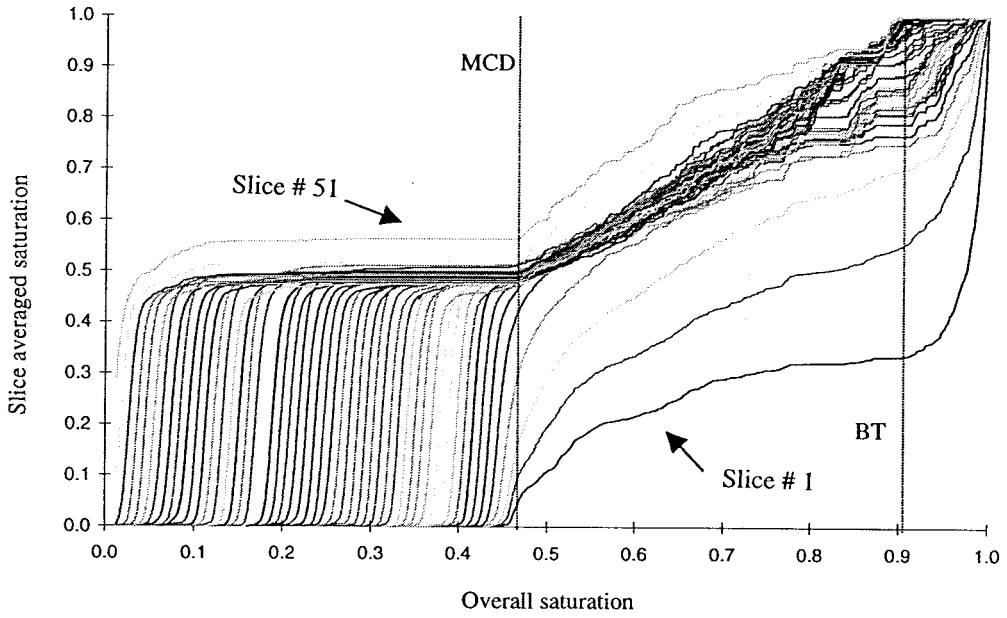

Fig. 5. Evolution of the slice averaged saturations as a function of the overall saturation. Each curve corresponds to a slice.

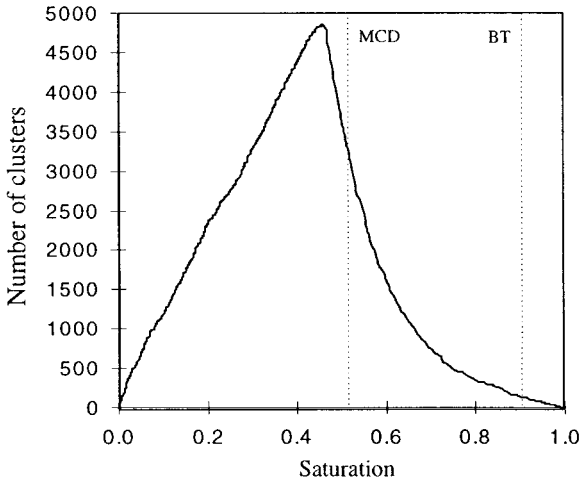

Fig. 6. Number of clusters as a function of the overall saturation.

butions for pure drainage (simulated by the standard invasion percolation algorithm) and for drying at BT and MCD (note that the main cluster is not taken into account in these figures). In these figures, the cluster size is expressed in numbers of sites. It can be seen that part of the clusters that form are eliminated in drying. However, in a first period, the number of clusters that form overcome the number of clusters that disappear due to evaporation. In a second period, the evaporation erosion process becomes dominant and the number of clusters diminishes up to the full drying of the network. Note also that the number of clusters that are present at BT is very small.

Fig. 8 shows the evolution of the extension along z of the largest clusters in the system. As can be seen from Fig. 8, the main cluster is at least one order of magnitude greater than the other clusters almost up to MCD. The homogeneous and isotropic nature of the invasion between BT and MCD is illustrated by the fact that the distribution of the disconnect clusters is more or less uniform along z (as those clusters mainly result from the fragmentation of the main clusters and this fragmentation can take place anywhere in the network, disconnect clusters are expected to form everywhere). After MCD, when there is no main cluster anymore for maintaining long distance connections within the liquid phase, the preferential erosion of the clusters located near the open face takes place as shown in Fig. 8. Additional information on the cluster evolution can be gained from the evolution of the liquid pore concentration profiles depicted in Fig. 9. The evolution of the fraction of pore in each slice that are liquid, or that belong to the main cluster, or that belong to the main cluster and are neighbor to at least one gas pore, are plotted in this figure. It can be seen that the fraction of pores that belong to isolated clusters is negligible at BT. This figure also confirms the fact that most of the pores occupied by liquid belong to the main cluster before MCD. The more and more ramified structure of the main cluster is clearly evidenced in Fig. 9 since at MCD most of the pore of the main cluster have at least one neighbor pore which is occupied by gas.

3.5. Drying curve

The network-drying curve is depicted in Fig. 10. Four main periods are observed. The first period that ends a little before BT is characterized by a rapid drop in the drying rate. It is interesting to note that this period, although with a less sharp fall in the drying rate, is observed in the experiment conducted by Maneval [3] for a pack of glass beads. Then, an almost constant rate period (CRP) is observed. The fourth period is a receding front period (RFP) that begins after MCD. Between the CRP and the RFP, a falling rate period (FRP) is observed. In the classical theory of drying [14], drying is divided in two periods: a constant rate period, and below a critical moisture content, a terminal period when the drying rate falls. As stressed by Keey [15], however, this classical conception does not account for the diversity of results reported in the literature. For instance, the fact that any very sharp discontinuity is observed between the CRP and the FRP in Fig. 10 is consistent with some of the drying curves for capillary porous media presented in [1] as well as with the drying curve measured by Maneval [3]. Keey notes also that the constant rate in the CRP is lower than the rate from a free surface. This is consistent with the rapid drop of the drying rate given by our model before the CRP starts. Such a rapid drop is not easy to determine experimentally since it occurs in the very early stage of drying.

To gain further insights into the mass transfer at the interface, the first slice average liquid vapor partial pressure, and the first slice average saturation were plotted in Fig. 11 together with the drying rate. The evolution of the standard deviation of the vapor partial pressure distribution in the first slice is also shown in Fig. 11. Not surprisingly, the (quasi) constant rate period is associated with a (quasi) constant average vapor partial pressure at the interface. More specifically, in a first phase up to BT, the average vapor partial pressure significantly decreases while the standard deviation increases markedly. The following phase is characterized by a much slower evolution of the average pressure and standard deviation. This phase corresponds to the CRP. During the FRP the standard deviation reaches a maximum around MCD. The FRP is also characterized by the average vapor partial pressure drop. The standard deviation decreases very

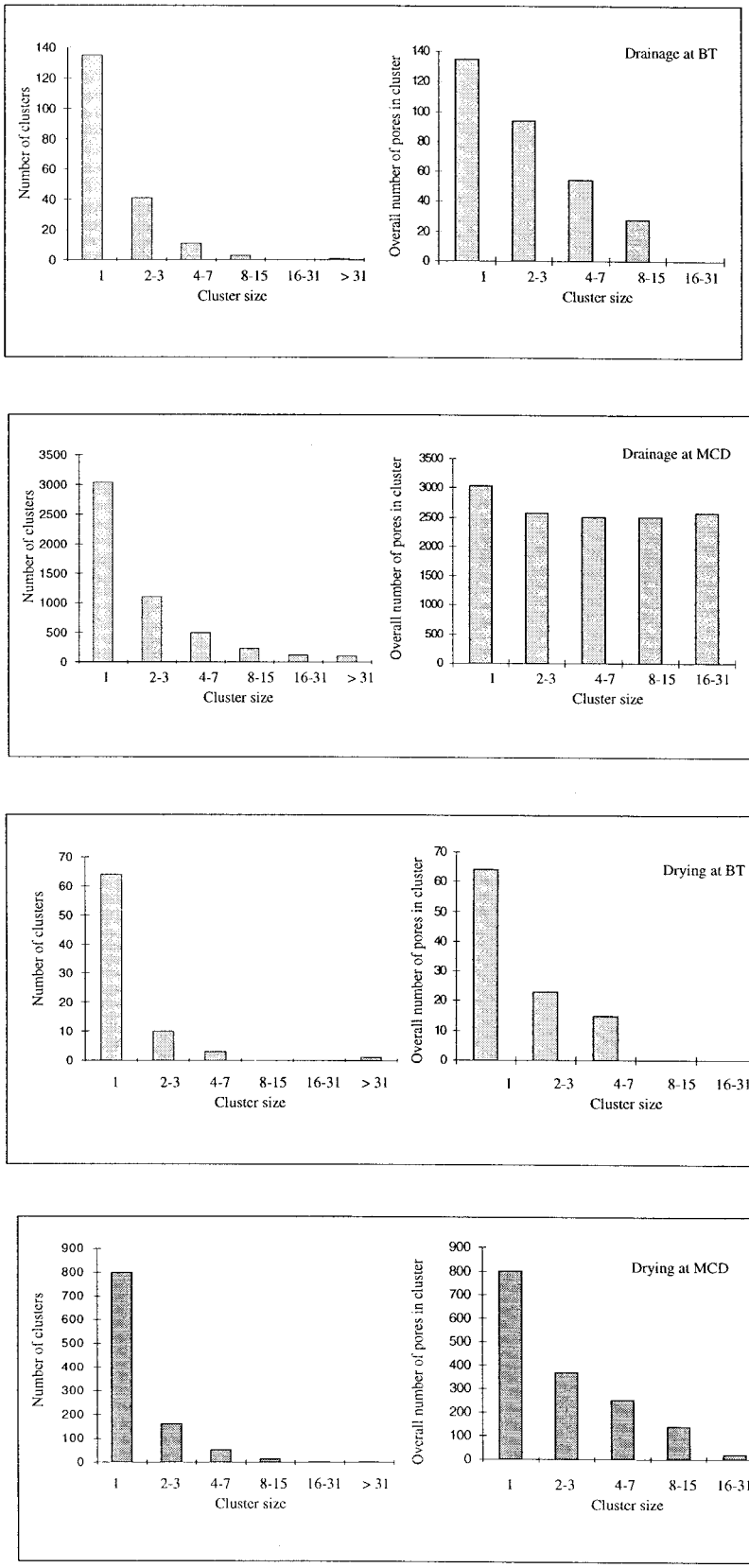

Fig. 7. Cluster distributions. Comparison between drainage and drying.

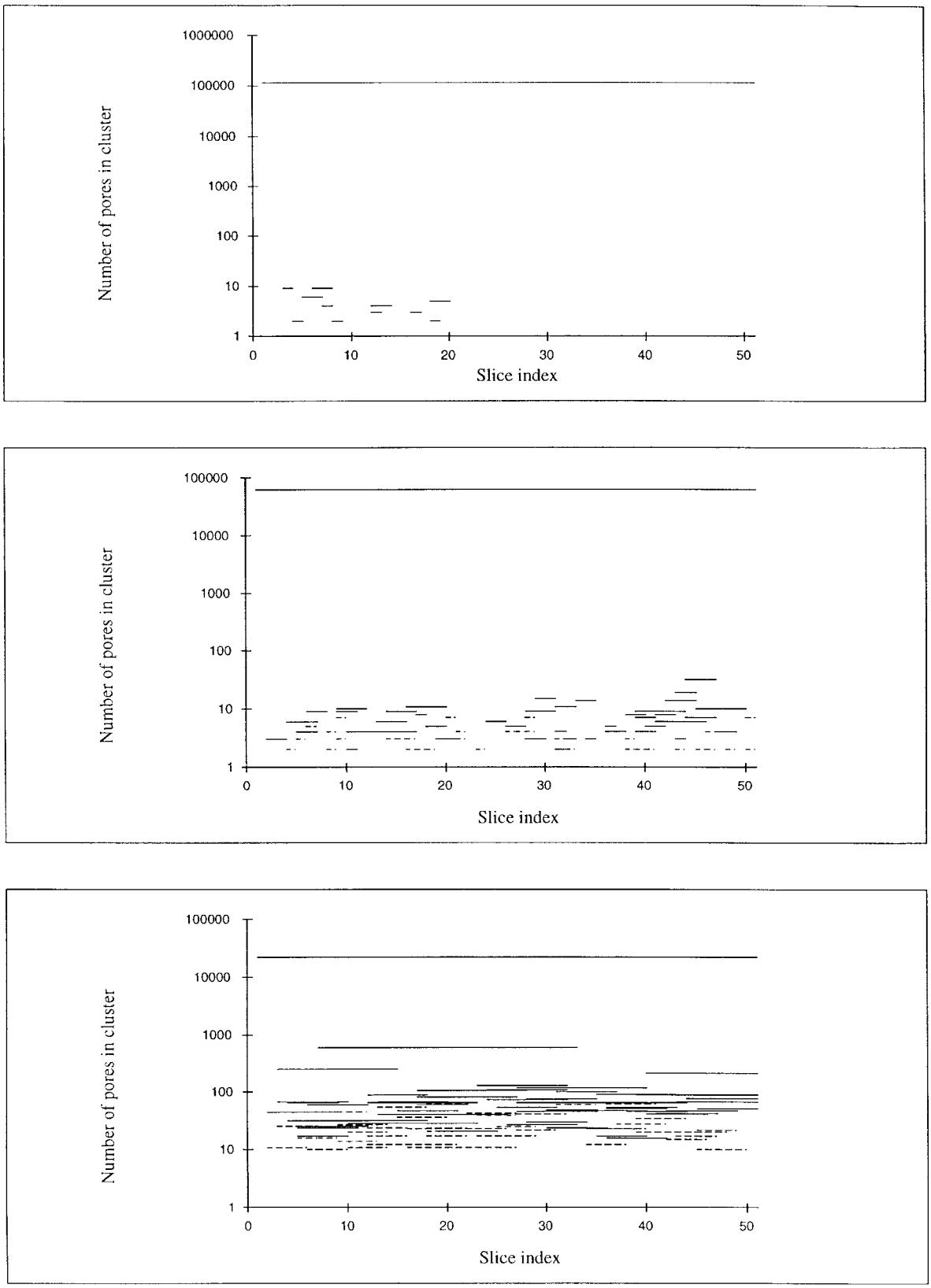

Fig. 8. Evolution of the cluster extension along z. Each line corresponds to one cluster.

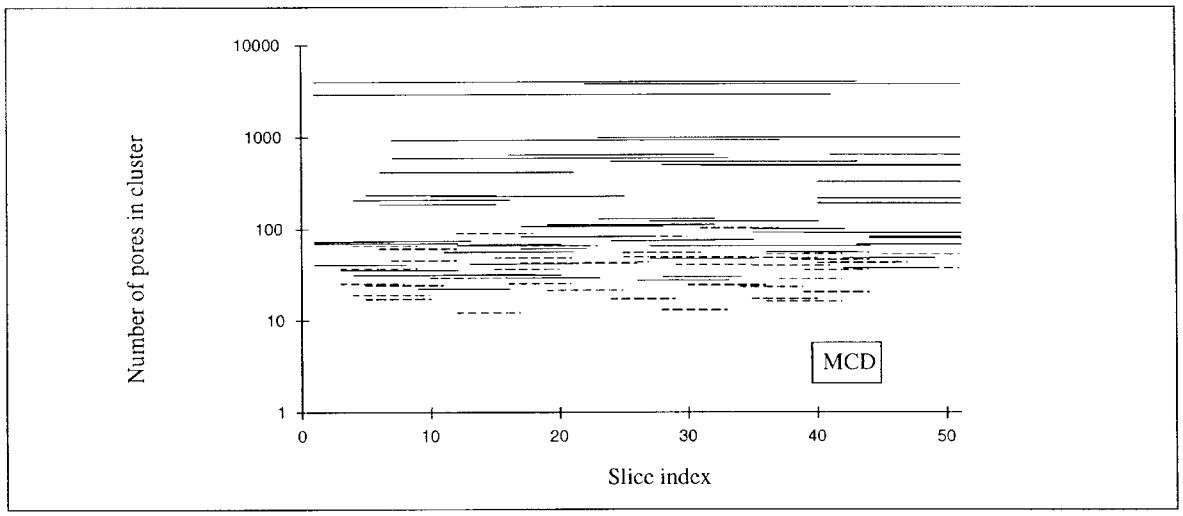

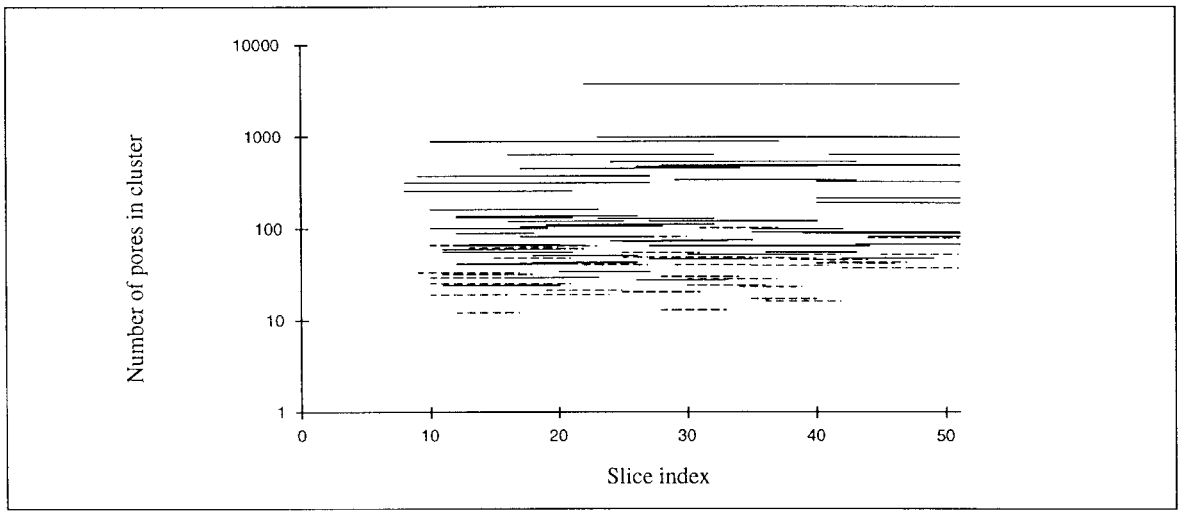

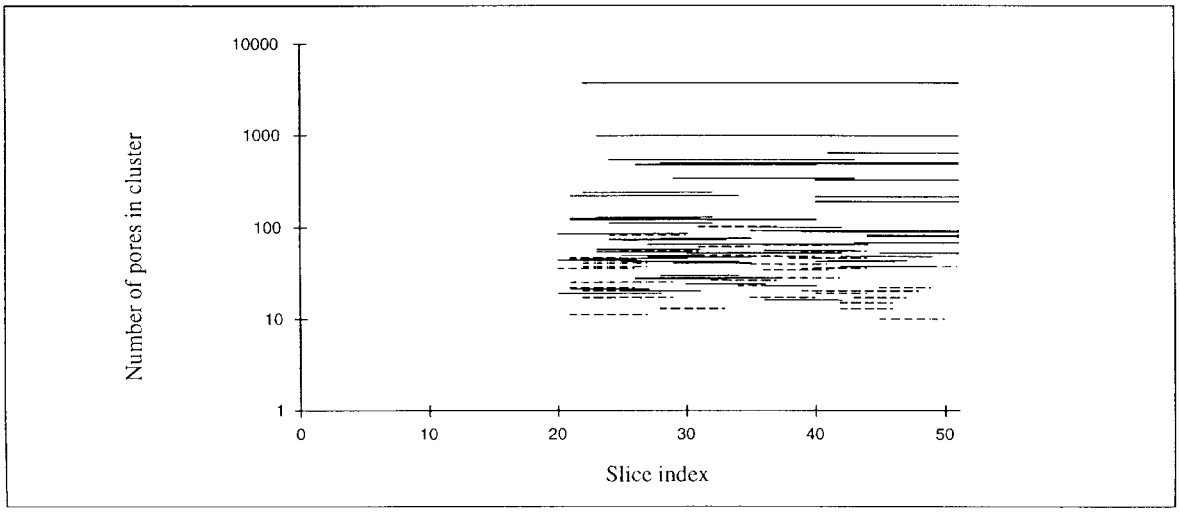

Fig. 8 (*continued*)

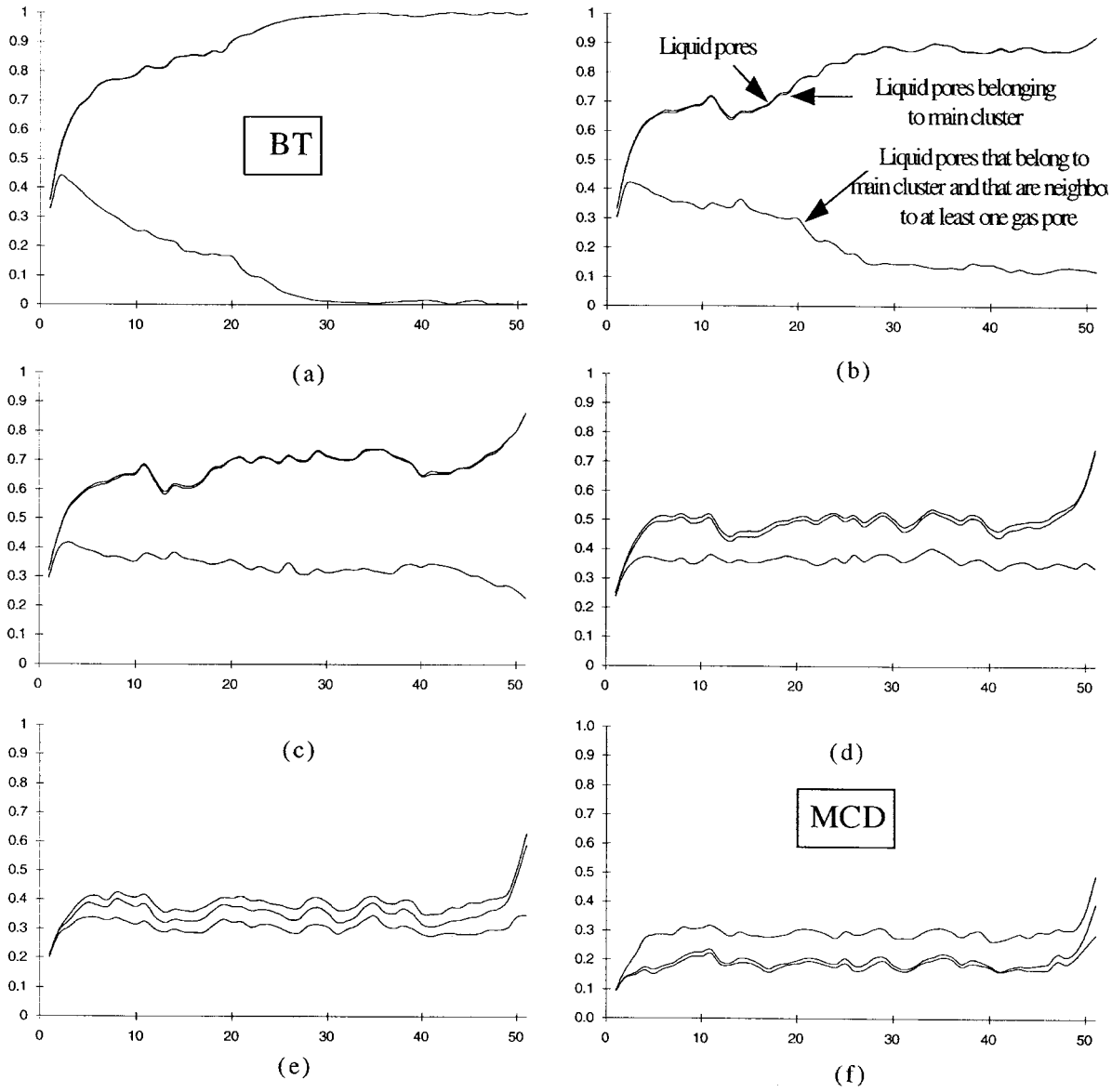

Fig. 9. Pore concentration profiles along z. $z = 1$ corresponds to the open face of network, $z = 51$ to the bottom face of network.

rapidly at the FRP-RCP transition and begins to tend gently towards zero (in the presence of a dry zone, diffusion makes the vapor partial pressure uniform at the interface).

4. Discussion

The main features of drying that are evident from the results obtained with the pore network model are the following: (1) drying can be divided in various periods, (2) drying periods can be distinguished from the drying curve and the evolution of various variables at the interface (average vapor partial pressure, average saturation in the first slice), and (3) drying periods can also be distinguished in terms of liquid phase structure within the network. The results indicate a strong correlation between the two series of drying periods but there are some subtleties. For the cubic system considered, BT and MCD may be considered as critical points in terms of liquid phase structuration. The transition between the first period and the quasi-constant rate period takes place close to BT. MCD marks the transition between the falling rate period

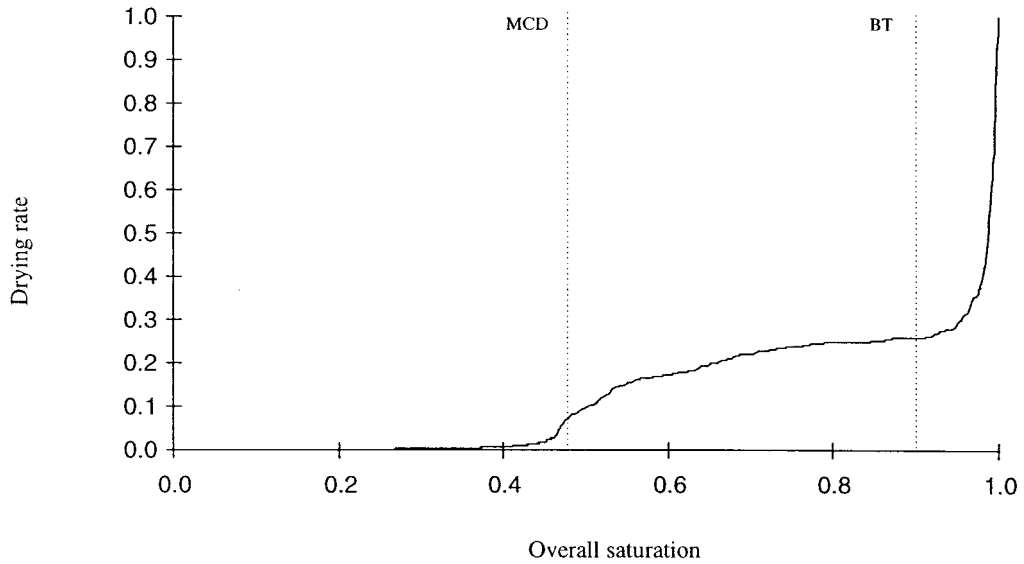

Fig. 10. Network drying curve (the drying rate is normalized by the drying rate at $t = 0$).

and the receding front period. The transition between the quasi constant rate period and the falling rate period is smooth and cannot be associated with some particular 'critical point'. This transition takes place between BT and MCD. During this phase (between BT and MCD), the liquid phase mainly belongs to the main cluster. The relative weight of the main cluster decreases during this phase that is characterized by the progressive fragmentation of the liquid phase. The main cluster maintains long distance connections in the liquid. This results in an essentially isotropic and homogeneous growth of the gas phase since due to the long distance connections invasion of a pore can take place everywhere in the network. As a consequence, the slice saturation becomes uniform in the bulk during this phase. Fig. 12 shows the evolution of the

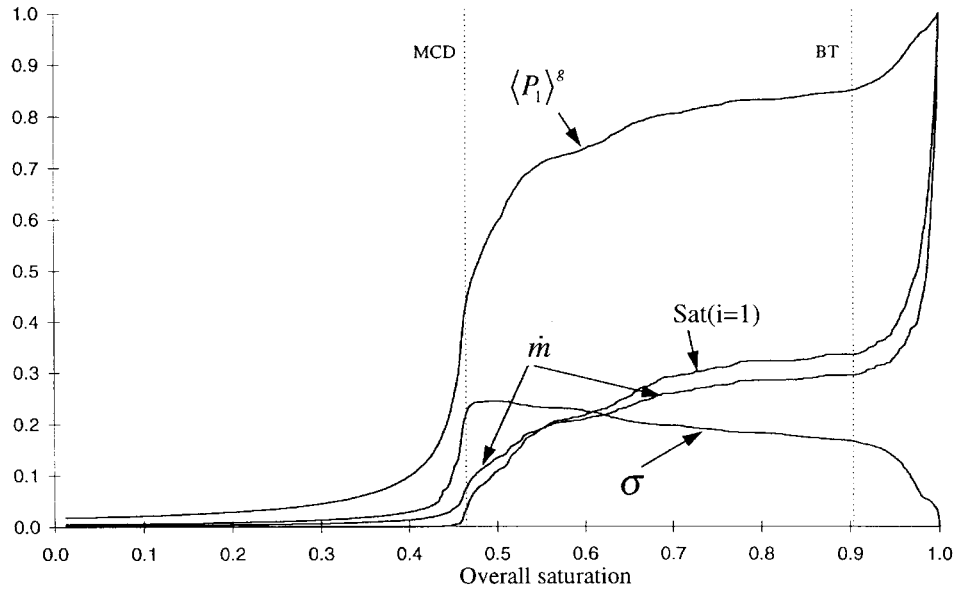

Fig. 11. Evolution of the average vapor partial pressure (normalized by the saturation vapor partial pressure) in the first slice, the standard deviation of the vapor partial pressure distribution in the first slice, the average saturation in the first slice and the drying rate as a function of the overall saturation.

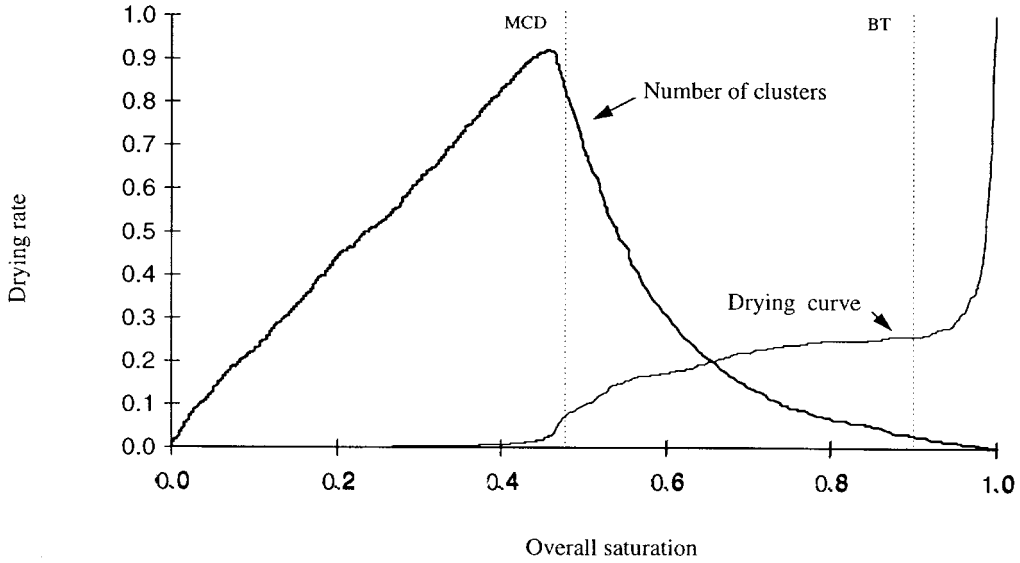

Fig. 12. Evolution of the number of clusters and the drying rate as a function of the overall saturation.

number of cluster and the drying curve. It can be seen that the transition between the CRP and the FRP is associated with a transition in the rate of cluster formation. Whereas, as explained before, the main cluster erosion can take place anywhere in the network, invasion of clusters of smaller size can only occur for clusters located near the open face (no evaporation takes place at the boundary of clusters located more deeply within the system before the RCP). The process of fragmentation of the liquid phase into clusters induces the preferential invasion of the clusters that forms in the open face region. Finally, the following description of the phase between BT and MCD can be proposed. Initially after BT, invasions essentially take place in the main cluster. Progressively, as more and more disconnected clusters form near the open face region, more and more invasions occur in these disconnected clusters leading to a decrease of the slice saturations more rapid at the interface than in the bulk as shown in Fig. 5. In this article, due to the intensive nature of the simulations, no exploration of the influence of the network size was attempted. However, we know from percolation theory that the percolation transition (here MCD) becomes sharper as the size of the system increases, Feder [16]. Therefore a sharper evolution of the drying curve around MCD is expected for large network.

Finally, the explanation of a CRP that comes out from these results is the following: the long distance connections within the main cluster and the fractal nature of the percolation cluster that forms in this capillarity controlled process allow the invasion in the bulk with almost no evolution of the saturation at the interface for a significant range of the overall saturation. As explained before, influence of the network size has not been studied here. However one expects that the number of pores in the bulk, that are occupied by gas and that are neighboring sites of liquid sites belonging to the main cluster, increases more rapidly with the size of the system than the number of sites at the interface (open face). At BT we know from the invasion percolation theory [10] that the number of sites (pores) belonging to the gas phase varies as $L^{2.5}$, where L is the size of the system (2.5 is the fractal dimension of the invader cluster in three dimensions). Most of these pores are neighbor to liquid pores. Therefore the ratio number of pores occupied by gas and neighbor to liquid sites/number of site at the interface may be expected to scale as $L^{0.5}$. Therefore, it is expected that the range of overall saturation for which a CRP is observed will increase with the network size. Two additional effects, which are not taken into account in the present model, can, however, be put forward as contributing factors to the occurrence of a CRP. First, the effect considered by Suzuki and Maeda [2], that is the fact that external transport along the interface contribute to homogenize the vapor partial pressures at the interface. Second, the influence of thin liquid film flows along the pore walls. This influence was investigated in Laurindo and Prat [7]. It was shown that the thin film flows along the roughness and corners of the pore walls can be a significant transport mechanism. In particular, film flows lead to a lower resistance to internal transport compared to pure diffusion and therefore contribute to maintain relatively higher partial pressure at the interface. It

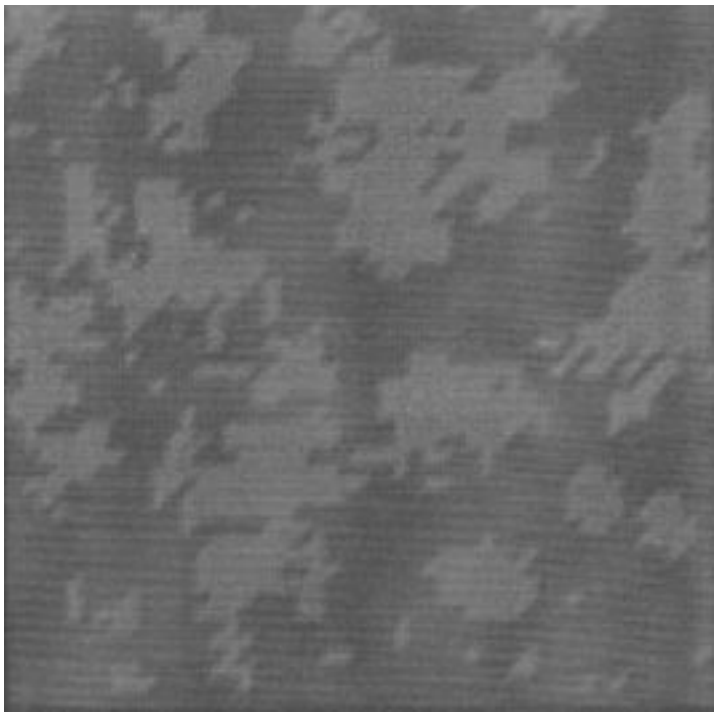

Fig. 13. Typical phase distribution in the first slice before MCD (dry patch phenomenon). Liquid in dark grey, gas in light grey.

was also shown in that article and its companion article, Laurindo and Prat [6], that film flows do not influence the main feature of the phase distribution as simulated by our pore network drying model.

It is also interesting to observe that the dry and wet patch phenomenon is captured by our model, as shown in Fig. 13. This result is in qualitative agreement with the results reported in [3]. In the context of the present model, dry patches are a consequence of the invasion percolation process, that is, an invasion process dominated by capillarity. It is perhaps worth mentioning that, in our model, the porous structure is macroscopically homogeneous (there is no correlation in the throat size distribution). Naturally, large scale structural heterogeneities (pore size correlation, variation of local porosity), that may be present in a real system, would certainly contribute to the formation of dry patches. However, our result clearly show that large-scale structural heterogenities are not necessary to observe dry patches. In the context of our model, dry patches may be considered as functional heterogeneities [17], since they are a consequence of the transport phenomenon itself. According to percolation theory, patches of any size can be expected at the interface during drying. In particular, and contrary to the assumption made by Van Brakel [1] for explaining the CRP on the basis of Suzuki and Maeda model, dry patches much larger than the pore size are therefore expected as shown in Fig. 13. A systematic study of the size and the evolution of the dry patches at the interface is, however, beyond the scope of the present article.

5. Conclusion

In this study, three-dimensional pore network simulations were used for studying drying of capillary porous media. This type of approach leads to detailed information on the various aspects of drying (phase distribution, drying rate) that cannot easily be obtained experimentally. This approach may be, therefore, thought as opening up new perspectives for a better understanding of drying. In this article, we revisited some of the most fundamental aspects of drying, such that the formation of dry and wet patches and the occurrence of the constant rate period. It has been shown that these features of drying were the outcome of the three-dimensional invasion percolation patterns that are typical of drying at low capillary numbers. The results presented in this article are, however, essentially qualitative and may be regarded as preliminary. Due to the intensive nature of the computations, only one realization of a $51 \times 51 \times 51$ network was considered. In particular, the influence of the network size has not been investigated.

The study was restricted to situations dominated by capillarity. We know from previous studies [5,6,18], that gravity and/or viscous effects impose an upper limit in the size of the clusters that form during drying. It would be interesting to study the influence of these effects on the drying curve. This could be done through three-dimensional pore network simulations without too much difficulties.

Our simulations also suggest that the aspect ratio of the porous sample should influence the drying curve. This could be the object of a specific study and comparisons with experiments could provide an excellent test of the pore network model of drying used in the present article. Influence of sample size would also deserve to be explored experimentally.

Acknowledgement

Financial support from Institut Français du Pétrole is gratefully acknowledged.

References

[1] J. Van Brakel, Mass transfer in convective drying, in: A.S. Mujumdar (Ed.), Advances in Drying, Hemisphere, New York, 1980, pp. 217–267.
[2] M. Suzuki, S. Maeda, On the mechanism of drying of granular bed—mass transfer from discontinuous source, J. Chem. Eng. Jpn 1 (1) (1968) 26–31.
[3] J. Maneval, Studies of moisture transport in unconsolidated porous media: use of NMR as an experimental probe, Ph.D. thesis, University of California at Davis 1991.
[4] M. Prat, Percolation model of drying under isothermal conditions in porous media, Int. J. of Multiphase Flow 19 (4) (1993) 691–704.
[5] M. Prat, Isothermal drying of non-hygroscopic capillary-porous materials as an invasion percolation process, Int. J. of Multiphase Flow 21 (5) (1995) 875–892.
[6] J.B. Laurindo, M. Prat, Numerical and experimental network study of evaporation in capillary porous media. Phase distributions, Chem. Eng. Sci. 51 (23) (1996) 5171–5185.
[7] J.B. Laurindo, M. Prat, Numerical and experimental network study of evaporation in capillary porous media. Drying rates, Chem. Eng. Sci. 53 (12) (1998) 2257–2269.
[8] J.B. Laurindo, Evaporation en milieu poreux. Etude expérimentale sur milieux-modèles et modélsation de type percolation, INPT Thesis, Toulouse, France 1996.
[9] Y. Le Bray, Contributions à l'étude du changement de phase liquide-vapeur en milieu poreux. Simulations numériques sur réseaux de pores. INPT Thesis, Toulouse, France 1997.
[10] D. Wilkinson, J.F. Willemsen, Invasion percolation: a new form of percolation theory, J. Phys. A Math. Gen. 16 (1983) 3365–3376.
[11] W. Masmoudi, M. Prat, Heat and mass transfer between a porous medium and a parallel external flow. Application to drying of capillary porous materials, Int. J. of Heat and Mass Trans. 34 (8) (1991) 1975–1989.
[12] D. Stauffer, A. Aharaony, Introduction to Percolation Theory, Taylor & Francis, London, 1992.
[13] M. Kaviany, M. Mittal, Funicular state in drying of a porous slab, Int. J. of Heat and Mass Trans. 30 (7) (1987) 1407–1418.
[14] N.H. Ceaglske, O.A. Hougen, Drying granular solids, Ind. Eng. Chem. 29 (1937) 805–813.
[15] R.B. Keey, Drying: Principles and Practice, Pergamon, Oxford, 1972.
[16] J. Feder, Fractals, Plenum Press, 1988.
[17] J.H. Cushman, An introduction to hierarchical porous media. Ch.1, in: J.H. Cushman (Ed.), Dynamics of Fluids in Hierarchical Porous Media, Academic Press, New York, 1990.
[18] T.M. Shaw, Drying as an immiscible displacement process with fluid counterflow, Phys. Rew. Lett. 59 (15) (1987) 1671–1674.